

Plasmon-enhanced solar energy conversion in organic bulk heterojunction photovoltaics

Anthony J. Morfa, Kathy L. Rowlen, Thomas H. Reilly, Manuel J. Romero, and Jao van de Lagemaat

Citation: *Appl. Phys. Lett.* **92**, 013504 (2008); doi: 10.1063/1.2823578

View online: <http://dx.doi.org/10.1063/1.2823578>

View Table of Contents: <http://apl.aip.org/resource/1/APPLAB/v92/i1>

Published by the [American Institute of Physics](http://www.aip.org).

Related Articles

Transparent conductive electrodes of mixed TiO_2 -x-indium tin oxide for organic photovoltaics

Appl. Phys. Lett. **100**, 213302 (2012)

Transparent conductive electrodes of mixed TiO_2 -x-indium tin oxide for organic photovoltaics

APL: Org. Electron. Photonics **5**, 115 (2012)

Near infrared up-conversion in organic photovoltaic devices using an efficient $\text{Yb}^{3+}:\text{Ho}^{3+}$ Co-doped $\text{Ln}_2\text{BaZnO}_5$ ($\text{Ln} = \text{Y}, \text{Gd}$) phosphor

J. Appl. Phys. **111**, 094502 (2012)

Selective emitters design and optimization for thermophotovoltaic applications

J. Appl. Phys. **111**, 084316 (2012)

Thermo-economic assessment of end user value in home and community scale renewable energy systems

J. Renewable Sustainable Energy **4**, 023117 (2012)

Additional information on *Appl. Phys. Lett.*

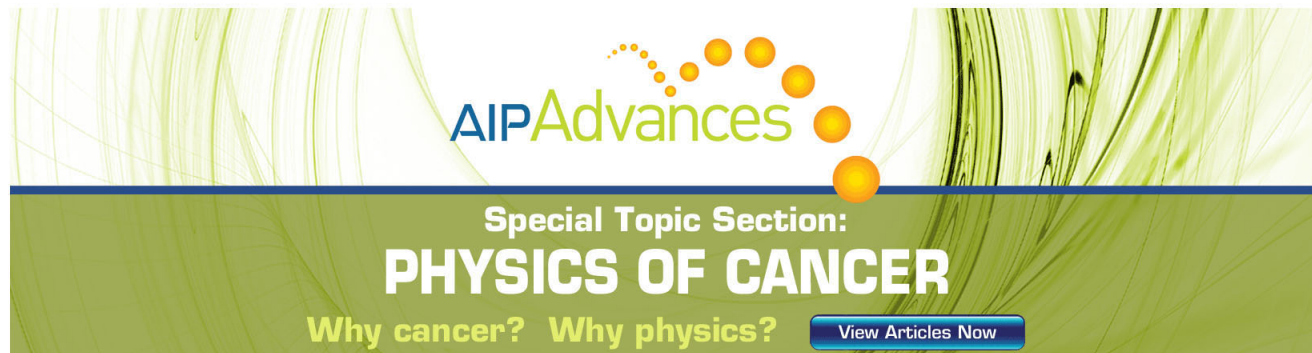
Journal Homepage: <http://apl.aip.org/>

Journal Information: http://apl.aip.org/about/about_the_journal

Top downloads: http://apl.aip.org/features/most_downloaded

Information for Authors: <http://apl.aip.org/authors>

ADVERTISEMENT

The advertisement features a green background with abstract, flowing lines. At the top, the 'AIP Advances' logo is displayed, with 'AIP' in blue and 'Advances' in green, accompanied by a series of orange dots. Below the logo, the text 'Special Topic Section: PHYSICS OF CANCER' is written in white, with 'PHYSICS OF CANCER' in a larger, bold font. At the bottom, the phrase 'Why cancer? Why physics?' is written in yellow, and a blue button with the text 'View Articles Now' is located on the right side.

AIP Advances

Special Topic Section:
PHYSICS OF CANCER

Why cancer? Why physics? [View Articles Now](#)

Plasmon-enhanced solar energy conversion in organic bulk heterojunction photovoltaics

Anthony J. Morfa and Kathy L. Rowlen^{a)}

Department of Chemistry and Biochemistry, University of Colorado, Boulder, Colorado 80309-0215, USA

Thomas H. Reilly III, Manuel J. Romero, and Jao van de Lagemaat^{b)}

National Renewable Energy Laboratory, 1617 Cole Boulevard, Golden, Colorado 80401-3393, USA

(Received 24 October 2007; accepted 19 November 2007; published online 3 January 2008)

Plasmon-active silver nanoparticle layers were included in solution-processed bulk-heterojunction solar cells. Nanoparticle layers were fabricated using vapor-phase deposition on indium tin oxide electrodes. Owing to the increase in optical electrical field inside the photoactive layer, the inclusion of such particle films lead to increased optical absorption and consequently increased photoconversion at solar-conversion relevant wavelengths. The resulting solar energy conversion efficiency for a bulk heterojunction photovoltaic device of poly(3-hexylthiophene)/[6,6]-phenyl C₆₁ butyric acid methyl ester was found to increase from 1.3% ± 0.2% to 2.2% ± 0.1% for devices employing thin plasmon-active layers. Based on six measurements, the improvement factor of 1.7 was demonstrated to be statistically significant. © 2008 American Institute of Physics.

[DOI: 10.1063/1.2823578]

Organic photovoltaic devices have been the focus of much work^{1–5} due to their potential as a low-cost source of renewable energy. Currently the highest published *certified* bulk heterojunction organic photovoltaic device is 4.4% efficient at air mass 1.5 (AM 1.5) illumination.⁴ The active layer for this device is a 1:1 mixture of poly(3-hexylthiophene) (P3HT) and [6,6]-phenyl C₆₁ butyric acid methyl ester (PCBM). During preparation of the P3HT:PCBM active layer, the mixture spontaneously phase segregates into interpenetrated domains, creating a bulk heterojunction (BHJ) device.² The electrical band gap of the absorber material is approximately 2.2 eV⁶ and its absorption threshold occurs approximately at 1.9 eV, too high to utilize the high-flux, red, and IR portion of the solar spectrum. Large gains in efficiency can be achieved by enhancing the device absorption at these wavelengths.

Surface plasmons are charge density waves with associated strongly enhanced electromagnetic fields occurring on the surface of certain metals.⁷ The enhanced local electromagnetic field has been utilized for surface-enhanced infrared absorption,^{8,9} and other techniques.^{10–16} Plasmonic materials have also been incorporated in semiconductor devices including light-emitting diodes,^{17,18} silicon photodiodes,^{19,20} and vacuum deposited thin film photovoltaics.^{21–28} Theoretical calculations have been performed to determine optimal plasmonic materials to enhance solar harvesting.²² Discontinuous Ag thin films provide an easy to fabricate, optically tunable surface plasmon active system. By varying average film thickness, discontinuous thin silver films have a surface plasmon resonance that can be tuned from the blue to the red portion of the visible spectrum.²⁹

Light is absorbed in the bulk heterojunction active layer, generating mainly excitons that dissociate into electrons and holes. Exciton dissociation takes place by charge separation between the electron donor, P3HT, and the electron acceptor, PCBM.³⁰ Since the dipole-allowed photogeneration of exci-

tons in the BHJ layer should scale with the electric field squared,³¹ we hypothesize that by enhancing the local electro-magnetic field with the inclusion of surface-plasmon active materials, enhancing the photogeneration of excitons in P3HT and, to a lesser degree, in PCBM is conceivable. Enhancements to the photogeneration of excitons would lead to a higher observable photocurrent from wavelengths near the plasmon resonance and into the red.

In this work, plasmonic enhancement of the P3HT:PCBM bulk heterojunction system is demonstrated in a spin-cast device with an incorporated thin vapor-deposited Ag film. Such films consist of coalesced plasmon active Ag islands.²⁹ The P3HT:PCBM system was chosen for its proven photovoltaic device efficiency and its ease of fabrication. Incorporation of a plasmon-active material is shown to enhance device efficiency by enhancing the short-circuit current. Mainly, enhancements to the external quantum efficiency at red wavelengths were observed. Previous studies of enhanced spectroscopic techniques near plasmon-active layers demonstrate that a considerable enhancement can be expected at distances that are relevant to our device configuration.^{32,33}

Samples were prepared as reported previously⁴ except that P3HT:PCBM films were spun at 1000 rpm and no annealing was performed. The deposition of Ag was performed once the chamber was evacuated to 5×10^{-8} torr. The deposition of Ag was performed at a rate of 0.2 Å/s with the total chamber pressure rising no higher than 8×10^{-8} torr. The Ag, purchased from Serac, was used as received. The final device structure with an incorporated plasmon-active Ag layer is shown schematically in Fig. 1. Silver film thicknesses of 1, 2, 3, and 4 nm were chosen to be sufficiently thin to limit the amount of light absorbed before reaching the active layer.²⁹ Solar conversion efficiencies were measured in nitrogen atmosphere on NREL's XT-10 simulator with its light intensity adjusted to account for solar mismatch. External quantum efficiencies were measured in nitrogen atmosphere using NREL's EQE user facility using a calibrated photodiode as a reference.

^{a)}Also at: InDevR, Inc., 2100 Central Ave., Boulder, Colorado 80301.

^{b)}Electronic mail: jao_vandelagemaat@nrel.gov.

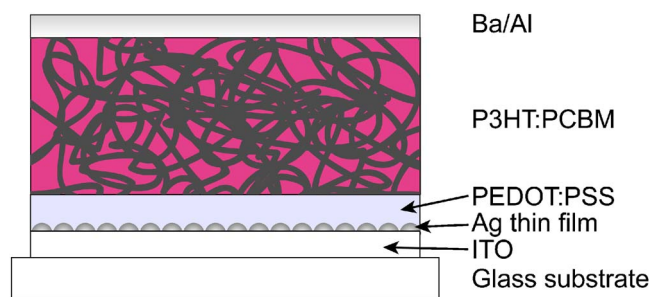


FIG. 1. (Color online) The device was fabricated with a thin silver film deposited onto ITO on a glass substrate. PEDOT:PSS was spun onto the silver layer followed by P3HT:PCBM and a barium/aluminum back electrode.

Figure 2 shows a field-emission scanning electron microscopy (FESEM) micrograph of a representative indium tin oxide (ITO) substrate with a 2 nm, by mass, discontinuous Ag film. The island nature of this film is apparent as the white dots on the grey background. The average island diameter for 2 and 4 nm thick films is 11.6 and 13.0 nm, respectively with both films having a median island diameter of 10.5 nm. These films are similar to previously reported plasmon-active films.²⁹

Tapping-mode atomic force microscopy (AFM) using a Digital Instruments Nanoscope IV multimode AFM showed that addition of Ag had no effect on the morphology of subsequently deposited poly(3,4-ethylenedioxythiophene) poly(styrenesulfonate) (PEDOT:PSS) layers. Samples with and without Ag included have an equal root-mean square roughness of 1.4 nm, much lower than that of the ITO substrate (5 nm).

In order to determine the effect of the plasmon-active layer on the exciton creation in the BHJ layer, current-voltage (*IV*) and incident photon-to-current conversion efficiency (IPCE) measurements were performed. Current-voltage measurements were performed under AM1.5 illumination. These values are lower than those previously demonstrated in the highest efficiency devices,⁴ but are consistent with the thinner active layer that is used here. The measured thickness of the BHJ layer is between 150 and 170 nm.

Figure 3 shows the average short-circuit current (J_{sc}) as a function of increasing nominal Ag film thickness. The samples for this study were spun from the same solutions of PEDOT:PSS and P3HT:PCBM, and averages were calculated from six devices on one plate for consistency. For a Ag film thickness of 1 nm, the average J_{sc} is 6.93 mA/cm². This is a factor of 1.49 increase over the average reference J_{sc} of

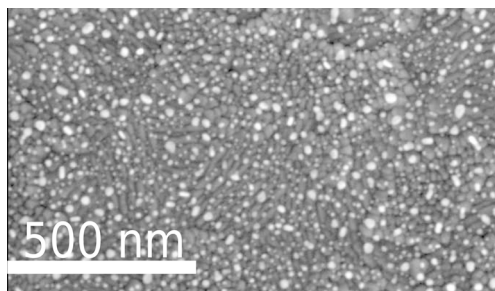


FIG. 2. FESEM micrograph of a representative 2 nm silver film on ITO. The white bar is approximately 500 nm in length.

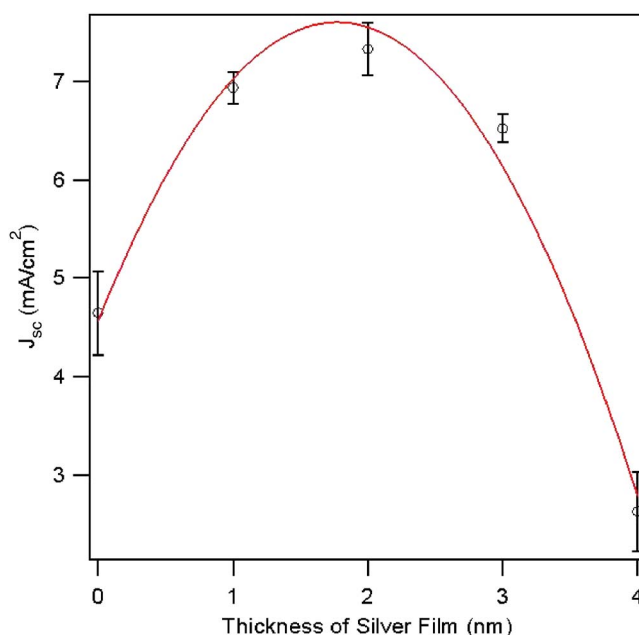


FIG. 3. (Color online) J_{sc} values plotted vs silver film thickness. The average J_{sc} value for six devices is marked with the \circ symbol, and the error bars are one standard deviation. The continuous (red) fit line is a second order polynomial used to guide the eye.

4.65 mA/cm². The highest increase to J_{sc} was observed for devices incorporating 2 nm of Ag. The average J_{sc} value was 7.33 mA/cm², a factor of 1.58 increase over the average reference value. The maximum J_{sc} observed was 7.71 mA/cm², a factor of 1.43 increase with respect to the maximum reference J_{sc} of 5.39 mA/cm². As the Ag film thickness was increased beyond 2 nm, a downward trend in J_{sc} was observed.

Table I shows an overview of the relevant average device parameters [J_{sc} , efficiency (η) and open-circuit voltage (V_{oc})] with their associated standard deviations. On average, the reference device and devices incorporating 1 nm of Ag were 1.31% and 2.23%, efficient, respectively. This corresponds to a factor of 1.70 increase. Beyond about 2 nm of silver, the efficiency decreases again. The V_{oc} decreases slightly with increasing silver coverage. This may be due to a decrease in work function of the transparent electrode.

The IPCE spectra are shown in Fig. 4. Two significant differences with respect to the reference are observed. The Ag samples exhibit a decrease in quantum efficiency at 450 nm. This feature coincides with the dip observed in the transmission spectra owing to the surface plasmon resonance of the Ag nanoparticles (not shown). At longer wavelengths (>500 nm), a strong increase in external quantum efficiency is observed in all silver samples, except that with a nominal

TABLE I. Average device parameters as a function of nominal silver film thickness. Errors reported as one standard deviation.

Ag height (nm)	J_{sc} (mA/cm ²)	η (%)	V_{oc} (mV)
0 (Ref)	4.6±0.4	1.3±0.2	566±5.6
1	6.9±0.2	2.2±0.1	590±5.8
2	7.3±0.3	2.1±0.1	581±8.8
3	6.5±0.1	1.8±0.2	564±30.9
4	2.6±0.4	0.9±0.1	599±6.2

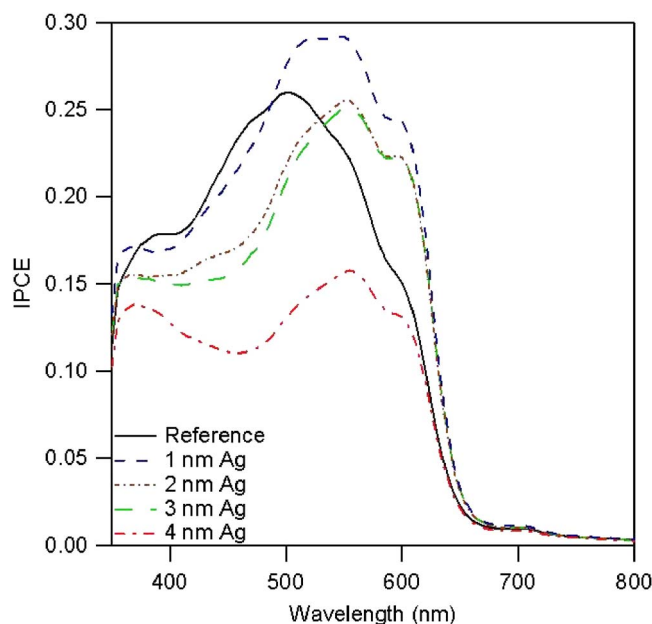


FIG. 4. (Color online) IPCE spectra of devices containing 1, 2, 3, and 4 nm silver films demonstrate the increased photocurrent at wavelengths over 500 nm. The strong absorption of the silver films on the IPCE is also seen as a dip centered near 450 nm.

thickness of 4 nm. This increase is the source of the increased short-circuit current and thus efficiency.

Placing the silver below the PEDOT:PSS layer proves to be important in determining the origin of the improvement to the devices with silver. Each device was made from the same solution of P3HT:PCBM to ensure similar active layer thickness and degree of morphological ordering. One can dismiss the possibility that an increase on the red shoulder of the IPCE spectra is associated with structural changes in the P3HT:PCBM films due to the PEDOT:PSS being spun as a barrier layer on top of the silver and the lack of morphological change as verified by AFM.

When PEDOT:PSS is annealed after being spin cast on thin Ag films, the IV curves show decreased device efficiency and nonideal diode behavior, this effect is still not understood. The film thickness of the PEDOT:PSS layer is another concern for these devices as the enhanced electromagnetic field decays rapidly with distance.³⁴ In this study, devices were solvent annealed with thin active layers, causing the red response to be low. It can be expected that optimized, annealed devices that already have a good red response will show a smaller relative increase in efficiency.³ It could be possible to enhance the subgap response of the cell even in optimally thick devices. This could be achieved by tuning the plasmon-enhancement wavelength further to the red than the currently presented layer. Tuning the plasmon resonance to lower energies can be achieved by using gold instead of silver or by annealing a thicker silver layer to form larger islands.

In summary, we have utilized plasmonic materials to create an organic photovoltaic structure with increased output current at long wavelengths. Further work to optimize the plasmon-enhanced bulk heterojunction is ongoing.

One of the authors, Anthony Morfa, acknowledges support from an NSF—IGERT fellowship. Financial support was also obtained from Airforce MURI Grant No. 153-6087. This work has been authored by an employee of the Midwest Research Institute under Contract No. DE-AC36-99GO10337 with the U.S. Department of Energy.

- ¹P. W. M. Blom, V. D. Mihailescu, L. J. A. Koster, and D. E. Markov, *Adv. Mater. (Weinheim, Ger.)* **19**, 1551 (2007).
- ²S. Gunes, H. Neugebauer, and N. S. Sariciftci, *Chem. Rev. (Washington, D.C.)* **107**, 1324 (2007).
- ³H. Kim, W. W. So, and S. J. Moon, *J. Korean Phys. Soc.* **48**, 441 (2006).
- ⁴G. Li, V. Shrotriya, J. S. Huang, Y. Yao, T. Moriarty, K. Emery, and Y. Yang, *Nat. Mater.* **4**, 864 (2005).
- ⁵J. Nelson, *Curr. Opin. Solid State Mater. Sci.* **6**, 87 (2002).
- ⁶M. Onoda, K. Tada, A. A. Zakhidov, and K. Yoshino, *Thin Solid Films* **331**, 76 (1998).
- ⁷H. Raether, *Surface-Plasmons on Smooth and Rough Surfaces and on Gratings* (Springer, Berlin, 1988), Vol. 88, p. 1.
- ⁸E. A. Carrasco-Flores, R. E. Clavijo, M. M. Campos-Vallette, and R. F. Aroca, *Appl. Spectrosc.* **58**, 555 (2004).
- ⁹T. R. Jensen, R. P. Van Duyne, S. A. Johnson, and V. A. Maroni, *Appl. Spectrosc.* **54**, 371 (2000).
- ¹⁰K. Kneipp, Y. Wang, H. Kneipp, L. T. Perelman, I. Itzkan, R. R. Dasari, and M. S. Feld, *Phys. Rev. Lett.* **78**, 1667 (1997).
- ¹¹M. Moskovits, *Rev. Mod. Phys.* **57**, 783 (1985).
- ¹²S. Nie and S. R. Emory, *Science* **275**, 1102 (1997).
- ¹³S. Wang, S. Boussaad, and N. J. Tao, *Rev. Sci. Instrum.* **72**, 3055 (2001).
- ¹⁴C. K. Chen, A. R. B. Decastro, and Y. R. Shen, *Phys. Rev. Lett.* **46**, 145 (1981).
- ¹⁵A. C. R. Pipino, G. C. Schatz, and R. P. Van Duyne, *Phys. Rev. B* **49**, 8320 (1994).
- ¹⁶O. Sgalli, I. Utke, P. Hoffmann, and F. Marquis-Weible, *J. Appl. Phys.* **92**, 1078 (2002).
- ¹⁷K. R. Catchpole and S. Pillai, *J. Lumin.* **121**, 315 (2006).
- ¹⁸S. Pillai, K. R. Catchpole, T. Trupke, G. Zhang, J. Zhao, and M. A. Green, *Appl. Phys. Lett.* **88**, 161102 (2006).
- ¹⁹S. H. Lim, W. Mar, P. Matheu, D. Derkacs, and E. T. Yu, *J. Appl. Phys.* **101**, 104309 (2007).
- ²⁰D. M. Schaadt, B. Feng, and E. T. Yu, *Appl. Phys. Lett.* **86**, 063106 (2005).
- ²¹C. Bonnand, J. Bellessa, and J. C. Plenet, *J. Non-Cryst. Solids* **352**, 1683 (2006).
- ²²J. R. Cole and N. J. Halas, *Appl. Phys. Lett.* **89**, 153120 (2006).
- ²³H. Dittlbacher, F. R. Aussenegg, J. R. Krenn, B. Lamprecht, G. Jakopic, and G. Leising, *Appl. Phys. Lett.* **89**, 161101 (2006).
- ²⁴S. Hayashi, K. Kozaru, and K. Yamamoto, *Solid State Commun.* **79**, 763 (1991).
- ²⁵J. K. Mapel, M. Singh, M. A. Baldo, and K. Celebi, *Appl. Phys. Lett.* **90**, 121102 (2007).
- ²⁶B. P. Rand, P. Peumans, and S. R. Forrest, *J. Appl. Phys.* **96**, 7519 (2004).
- ²⁷O. Stenzel, A. Stendal, K. Voigtsberger, and C. Vonborczyskowski, *Sol. Energy Mater. Sol. Cells* **37**, 337 (1995).
- ²⁸M. Westphalen, U. Kreibitz, J. Rostalski, H. Luth, and D. Meissner, *Sol. Energy Mater. Sol. Cells* **61**, 97 (2000).
- ²⁹R. Gupta, M. J. Dyer, and W. A. Weimer, *J. Appl. Phys.* **92**, 5264 (2002).
- ³⁰Y. Kim, S. Cook, S. M. Tuladhar, S. A. Choulis, J. Nelson, J. A. Durrant, D. D. C. Bradley, M. Giles, I. McCulloch, C. S. Ha, and M. Ree, *Nat. Mater.* **5**, 197 (2006).
- ³¹A. Luque and S. Hegedus, *Handbook of Photovoltaic Science and Engineering* (Wiley, Hoboken, NJ, 2003), Vol. 1, p. 1138.
- ³²A. J. Haes, S. L. Zou, G. C. Schatz, and R. P. Van Duyne, *J. Phys. Chem. B* **108**, 6961 (2004).
- ³³H. Knobloch, H. Brunner, A. Leitner, F. Aussenegg, and W. Knoll, *J. Phys. Chem. B* **98**, 10093 (1993).
- ³⁴D. D. Evanoff, R. L. White, and G. Chumanov, *J. Phys. Chem. B* **108**, 1522 (2004).